

Document downloaded from:

<http://hdl.handle.net/10251/95449>

This paper must be cited as:

Ferrer Giménez, C.; Pascual Guillamón, M.; Busquets Mataix, DJ.; E. Rayón (2010). Tribological study of FeCuCrgraphite alloy and cast iron railway brake shoes. *Wear*. 268(5):784-789. doi:10.1016/j.wear.2009.12.014



The final publication is available at

<http://doi.org/10.1016/j.wear.2009.12.014>

Copyright Elsevier

Additional Information

Tribological study of Fe-Cu-Cr-graphite alloy and cast iron railway brake shoes by pin-on-disc technique

C. Ferrer, M. Pascual, D. Busquets, E. Rayón*

Instituto de Tecnología de Materiales, Universidad Politécnica de Valencia.

Camí de Vera s/n. E-46022. Valencia, Spain

*emraen@upvnet.upv.es

CORRESPONDING AUTHOR:

Ph.D. Emilio Rayón Encinas

Tel. +34 667238511

FAX: +34 963877629

E-mail: emraen@upvnet.upv.es

Abstract

A new class of materials is being installed in railway brake blocks to substitute classic cast iron in order to reduce the rolling noise produced by the roughness of the tread-wheel surface. The tribological properties of cast iron and Fe-Cu-Cr-graphite sintered alloy brake shoes were analyzed. Kinetic friction coefficient (μ) and wear were monitored by means of a pin-on-disc technique. The sintered alloy brake showed an increase in μ at higher braking velocities while the cast iron brake exhibited a decrease in μ . Wear was greater on the sintered alloy, explained by its low shear strength which decreased due to its low thermal conductivity. The roughness produced by the sintered brake shoes in wheel tread surface was 10 times lower than that produced by cast iron.

Keywords: Sliding friction, surface topography, cast iron, sintered alloy, brakes, pin-on-disc

1. Introduction

Noise elimination is an issue that is gaining importance on railways. At present, an estimate of one million people in Europe have to be protected from railway noise, by noise barriers and by noise-insulated buildings [1,2]. One of the main sources of railway noise is rolling noise arising from the contact between the wheels and the tracks.

Rolling noise is the dominant source of noise at speeds between 60 km/h and 200-250 km/h [3,4]. Rough wheels and rough tracks increase the noise emission. Thus, the rougher the wheel surface, the greater the noise produced. Other sources of noise such as aerodynamic friction are only important when high velocities are reached (more than 300 km/h).

The simplest way to reduce the velocity of a railway in motion is through the friction produced between a brake shoe and the wagons' wheel tread. Cast iron (usually as a gray cast iron) has been the most used material in brake shoes [5]. Cast iron brake shoes have the disadvantage of making the wheel tread surface rougher during braking [6]. Thus, a reduction in noise should be achievable through the substitution of cast iron brake shoes by other material leading to lower wheel surface roughness.

In fact, over the last years, cast iron shoes have been replaced by composite synthetic brake shoes. It has been demonstrated that cast iron brake shoes make the wheel surface much rougher than a similar product made with a composite material. Replacing the cast iron shoes with a synthetic product can therefore substantially reduce the wagon noise

emissions, for example, by about 10 dB for a 100 km/h freight train [6]. Nevertheless, previous experiences using a polymeric composite brake demonstrated that the organic material can be burned, coating the wheel-tread with an organic film. This film diminishes the friction between the wheel tread and rail or brake shoe [8]. Other sintered alloys have been used as an Fe-Cu-Cr-Sn-graphite alloy [9]. These brake shoes exhibited a better braking behavior with less wear on the tread wheel. However, premature wear has been observed in this material, being less cost-effective.

The aim of this work is to study and compare the tribological properties of a gray cast iron brake and a composite sintered alloy brake (Fe-Cu-Cr-Sn-graphite). A pin-on-disc technique is proposed to analyze comparatively the friction coefficient of both materials. Other mechanical analysis and photothermal techniques were performed to discuss the wear phenomena.

2. Experimental set-up

The samples used in this work were extracted directly from the commercial brake shoes of a locomotive train. Microstructure and chemical composition were analyzed by standard metallographic and energy dispersive X-ray analysis (EDX) on a SEM respectively. The sintered alloy sample showed a composition of 38 % Cu, 34% Fe, 3% Cr, 15% C, 4% Sn, 4% O and 2% Al. Graphite, bronze and α -alumina were detected. The cast iron brake shoe showed a gray cast iron structure with graphite sheets in a perlite matrix. Standard compression testing showed a stress limit at 350 MPa, which corresponds to EN-GJL-300 standard. The Brinell hardness value measured for this material was 223 HB. On the other hand, a Brinell hardness value of 39 HB and

compressive strength of 45 MPa was obtained for the sintered alloy. All measures were carried out at room temperature.

2.1. Friction testing

Although Pin-on-disc technique does not describe the contact geometry, applied normal pressure and asperity distribution of wheel-tread, this technique is useful in the comparative tribological study of both materials. In fact, this technique allows the measurement of the kinetic friction and wear when a plate (the disc) of one material rolls in contact with a sample (the pin) of another material which can provide valuable information on the tribological behavior of both systems. Therefore, the aim of this study is the comparative study of two materials rather than replication of a real braking condition.

The test apparatus and testing technique is described as follows. MicroTest® pin-on-disc equipment was used to measure the wear and friction coefficient between the brake sample (cast iron or sintered alloy pin) and the steel plate (as the train wheel). A load of between 10 N and 500 N and angular velocities ranging from 10 r.p.m. to 500 r.p.m. can be programmed by a computer. The friction is then calculated and recorded in the computer by means of several sensors installed on the rotary's axis plate.

Figure 1 shows the Microtest pin-on-disc used. The following can be distinguished in the photograph: the plate (1), which moved the wheel sample (2) against the pin (3). Weights (4), which apply the contact force and a magnetic sensor (5) to measure the vertical movement of the arm, thus obtaining the wear of the pin.

The wheel sample was composed of the same material as the steel wheel railway with a composition of: 0.56% C, 0.4 % Si, 0.8 % Mn, 0.035% P, 0.035% S, 0.3% Cr, 0.3% Cu, 0.08% Mo, 0.3% Ni, 0.05% V and 0.4% Ti. The plate was polished until an average roughness value of $Ra=0.015 \mu\text{m}$ was achieved on both sides. One side of the plate was used for the cast iron pin test and the other side was used to perform the sintered alloy pin test.

The parameters selected for our experiments were loads of 10 N (0.2 Mpa) and 20 N (0.4 MPa) and velocities of 0.31 ms^{-1} and 1.05 ms^{-1} .

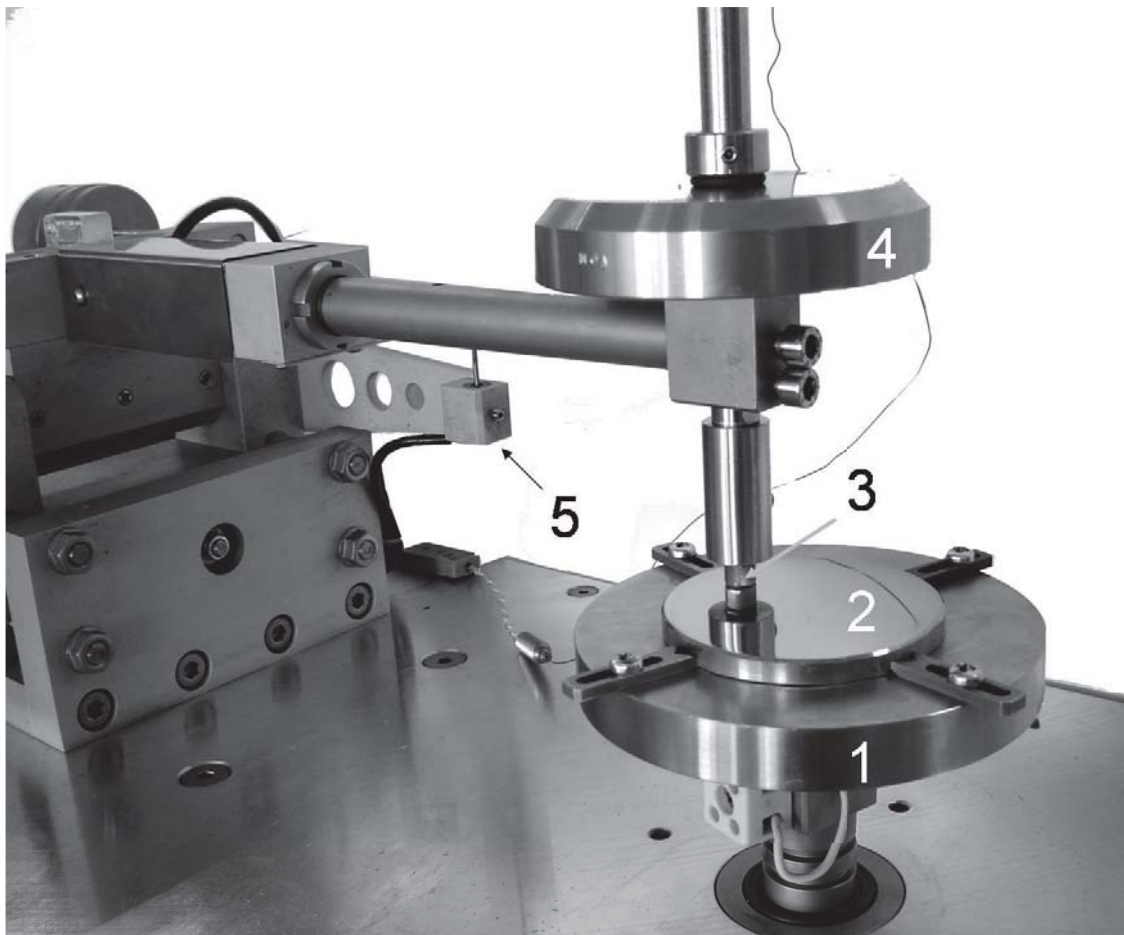


Figure 1. Photography of Microtest[®] pin-on-disc technique used. (1) Disc which rolled at programmed velocity. (2) Steel disc sample extracted from locomotive wheel. (3)

Sintered alloy or cast iron pin extracted from locomotive brake shoes. (4) Weights used to apply the braking contact force and (5) magnetic sensor to measure the wear.

2.2. Thermal analysis

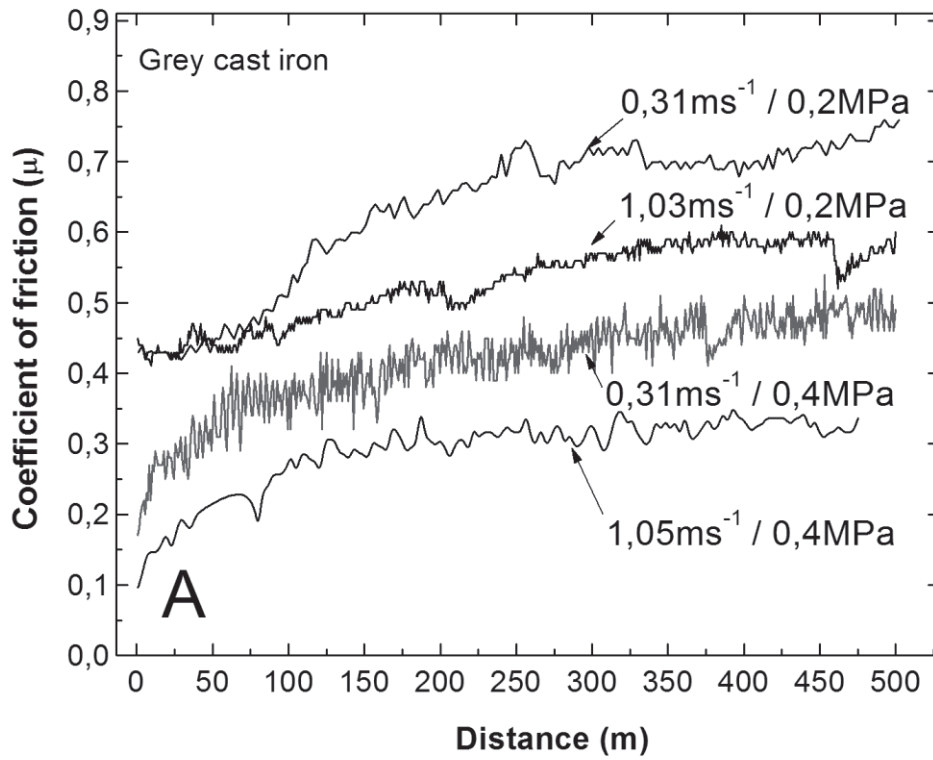
The thermal study of the brake materials is interesting from the point of view of the power dissipation capacity of each material. Thermal studies for both materials were performed using a Flir Systems ThermoCAM™ S65 infrared camera. Again, samples were extracted from a commercial brake shoe. Pieces 11x11x40 mm in size were then installed on a cylinder with large mass made of steel at 25 °C. With the large mass of the cylinder, we assumed the brake's holder to have good thermal dissipation. A cylindrical steel piece preheated to 500° C as a means to simulate the heat released during braking was placed on top of the sample at the same moment that the images began to be recorded every 5 seconds. The initial temperature conditions were the same for all of the samples and experiments.

3. Results

3.1. Tribological results

The friction coefficient μ were recorded for both brake materials sliding above the steel plate. Figure 2A shows the μ for cast iron and figure 2B shows the μ for sintered alloy. Cast iron curves showed that μ increased during the experiments regardless of the load conditions and velocities studied, unlike sintered alloy, which exhibited a more stable coefficient.

Braking pressures of 0.2 MPa and 0.4 MPa and velocities of 0.31ms^{-1} and 1.03ms^{-1} were tested. The average friction coefficients for these conditions are summarized in Figure 3 for clearer presentation.



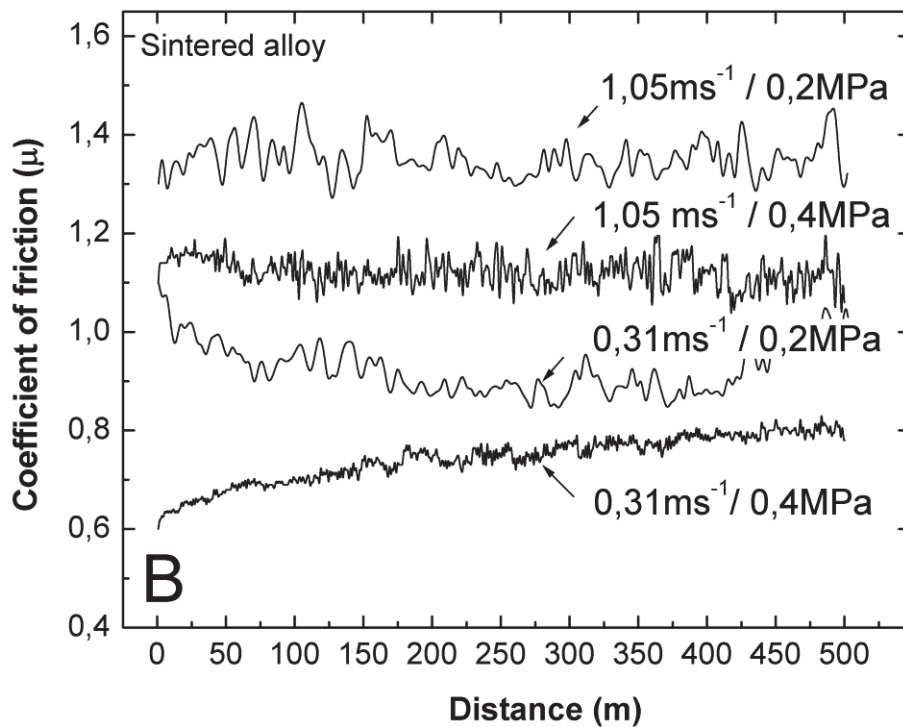


Figure 2. Kinetic friction coefficients (μ) at velocities of $0.3 \text{ ms}^{-1}/1\text{ms}^{-1}$ and under $0.2 \text{ MPa}/0.4\text{MPa}$ contact pressures. (A) Cast iron results and (B) sintered alloy Fe-Cu-Cr-graphite results.

The cast iron results showed that when the braking pressure was increased from 0.2 MPa to 0.4 MPa , the friction coefficients decreased from 0.55 to 0.25 at 1.03 ms^{-1} and from 0.7 to 0.4 at 0.3ms^{-1} . Moreover, when the velocity was increased from 0.3 ms^{-1} to 1.03 ms^{-1} , the friction coefficient decreased from 0.7 to 0.55 under pressures of 0.2 MPa and from 0.4 to 0.25 under pressures of 0.4 MPa . Thus, the cast-iron brake shoe sample presented two specific characteristics: (i) the higher the speed, the lower the friction coefficient and (ii) the higher the contact force of the brake shoe on the wheel, the lower the friction coefficient. These results agree with previously published reports [10,11]. In fact, both of these characteristics led to specific brake system designs for vehicles braked with cast iron shoes. This included reducing the brake cylinder pressure at low

speeds to prevent the wheels from locking, and equipping vehicles with twin or even triple brake blocks to prevent the specific application force from becoming too great and, as a result, the friction coefficient from becoming too low.

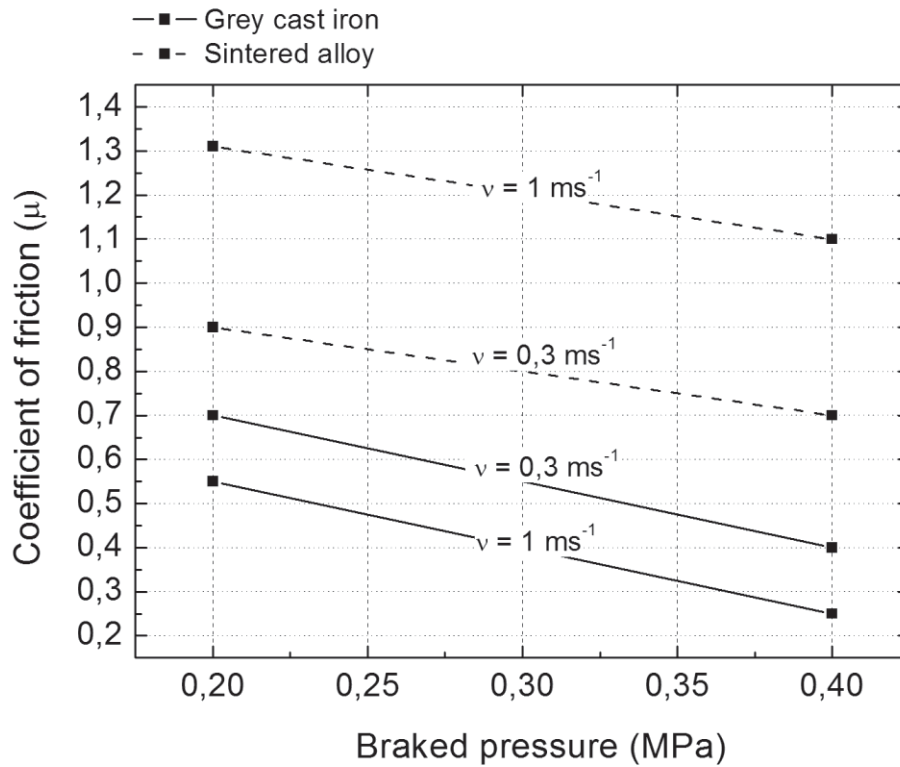


Figure 3. Coefficient of friction (μ) versus braking pressure at 1 ms^{-1} and 0.3 ms^{-1} for the cast iron and sintered alloy pin-on-disc results.

Kinetic friction results for sintered alloy showed a very stable μ coefficient along the 500 m distance tested. Average μ was 80% higher than that of the cast iron results. The μ behavior under the pressures tested was similar to that of the cast iron: when the pressure was increased from 0.2 MPa to 0.4 MPa, μ decreased from 0.9 to 0.7 at 0.3 ms^{-1} and from 1.3 to 1.1 at 1 ms^{-1} . Nevertheless, at higher velocities μ was higher: from 0.3 ms^{-1} to 1.03 ms^{-1} , μ increased from 0.9 to 1.3 under 0.2 MPa and from 0.7 to 1.1 under 0.4 MPa. These results must be taken into account when designing the brake system in

railway transport because, in this way, equivalent speeds must produce equivalent stopping distances. The rules which drive these behaviors will be discussed further below.

During friction analysis, wear and temperature were also measured and recorded. Wear was measured as vertical movement of the tribometer arm as a result of groove formation and thus represented in millimeters. The temperature reached in the sample was monitored by a thermocouple installed 10 mm from the sample contact surface. Although it was impossible to measure the temperature of the surface friction with a thermocouple, temperature curves gave an idea of the moment in which the power generated by the friction changed and therefore, also provided the mechanism which governed the friction and wear process.

No wear was detected at a sliding velocity of 0.3 ms^{-1} for both pressures and materials. In these cases the noise level recorded was very high compared to the wear signal. In addition, it was difficult to detect wear by the loss of weight method after the experiments made at 0.3 ms^{-1} due to the low wear produced. It was only possible to monitor a clear wear when a velocity of 1 ms^{-1} was tested. These observations indicated that sliding velocity was determinant in the wear process. Figure 4 shows the wear and temperature curves recorded for both shoe materials when the plate was rolling at 1 ms^{-1} . Wear in the cast iron sample followed a linear and thus a constant behavior after testing 100 meters. Temperature was also constant and reached $110 \text{ }^\circ\text{C}$. However, in the sintered alloy sample, the temperature increased very quickly after 100 meters and the wear process developed exponentially when it reached $170 \text{ }^\circ\text{C}$. However, one must bear in mind that temperatures measured are not necessarily the same on the contact surface.

After 500 meters of testing for the sintered alloy, the wear level reached 4.5 mm with respect to the 2.25 mm measured for the cast iron.

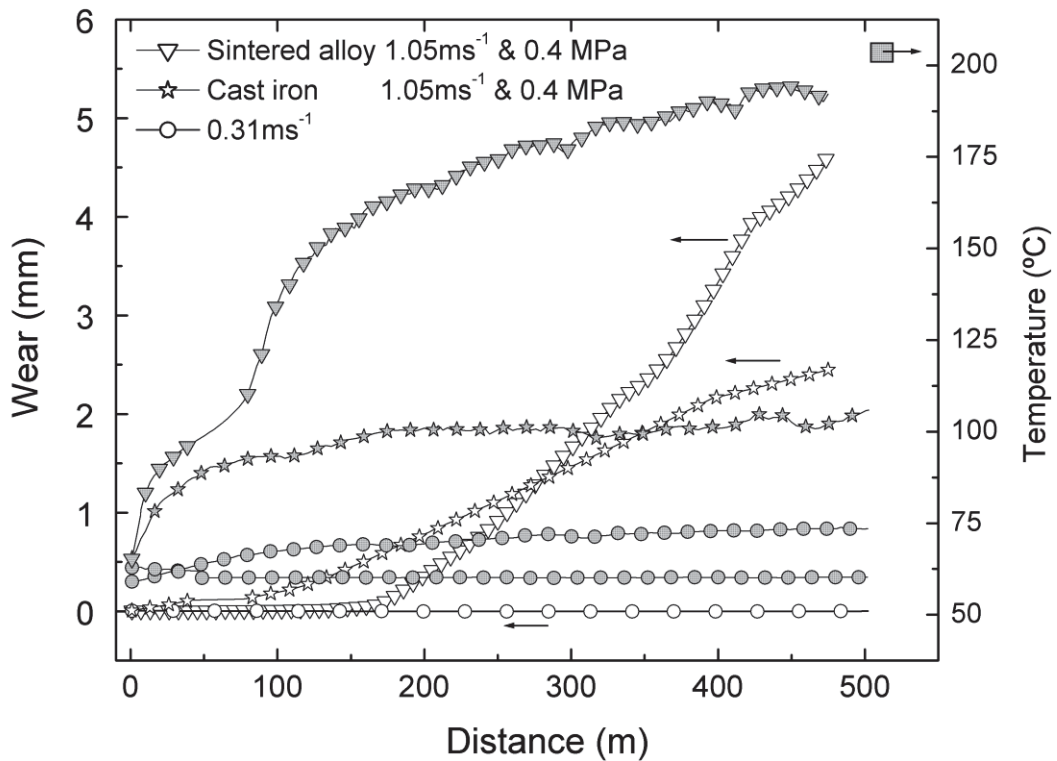


Figure 4. Wear and temperature results for cast iron and a sintered alloy versus distance tested.

In order to establish the roughness generated on the wheel surface by each shoe material, the plate was initially polished down to $0.145 \mu\text{m}$ (R_a), as measured by a perthometer M2 roughness tester. One side was used as sliding contact with the cast iron and the opposite side with the sintered alloy sample. The resulting roughness produced by wear was measured after all of the experiments for each material. Results showed a plate tread surface roughness of $1.635 \mu\text{m}$ for cast iron. However, the side used in contact with the sintered alloy practically did not show any changes with respect to the parent roughness, with a measured average roughness of $0.155 \mu\text{m}$. Although R_a gives no indication of change in surface topography (which is expected to have taken

place), as differences in roughness of one order of magnitude have been measured the higher roughness produced with using cast iron pads as mentioned before is corroborated. Sintered alloy, softer and with a graphite flakes that act as lubricant, made less erosion on the tread surface, maintaining a high friction coefficient value. This decrease in roughness on the tread surface will translate into a lower rolling noise.

3.2. Thermal results

Friction dissipates energy in the form of heat. The combination of braking effort through friction between the brake shoe and the wheel tread surface produces thermal and contact stresses on the wheel, which often result in wheel damage. High thermal and contact stresses are known to initiate microcracks in the wheel tread, eventually leading to a defect condition known as shelling. In addition, the heat accumulated in the brake shoe decreases the shear strength, causing premature wear due to delamination of the brake surface. Around 25% to 30% of the friction heat produced during braking is currently dissipated by the brake shoe [12]; the rest by the wheel. The wheels must therefore be able to deal with this greater proportion of energy. For all of these reasons, the thermal dissipation produced in the braking material must be analyzed.

Two types of thermal measurements were performed, (i) by means of a thermocouple inserted in the sample during pin-on-disc testing (ii) and by means of an infrared camera when the sample was heated with a preheated mass. In the first case, the temperature observed (figure 4) when the wheel was sliding on the brake sample reached 110°C in the gray cast iron at the maximum velocity and pressure tested (1ms^{-1} and 0.4 MPa). Under the same conditions, the sintered alloy reached 190°C. At lower velocities and forces, the temperature did not reach 50°C for any material. These results gave a first

indication that velocity is the most influential parameter on the maximum temperature reached. Thermal conductivity of the alloy was lower than that of the cast iron as shown in figure 5 by an infrared image sequence of (A) sintered alloy and (B) gray cast iron samples when a preheated steel mass was installed on top of the samples. Initial conditions have not been represented due to the homogeneous blue color of the image at 35°C, which made it difficult to observe a clear image. The colored background was due to the irradiation heat flux of the heated sample. Images showed that the map of temperatures was very similar during the first 45 seconds of the heating process. Only after 65 seconds did the cast iron sample show a higher (more than 210°C) in-depth heating. Sintered alloy was colder in-depth for the same time reached.

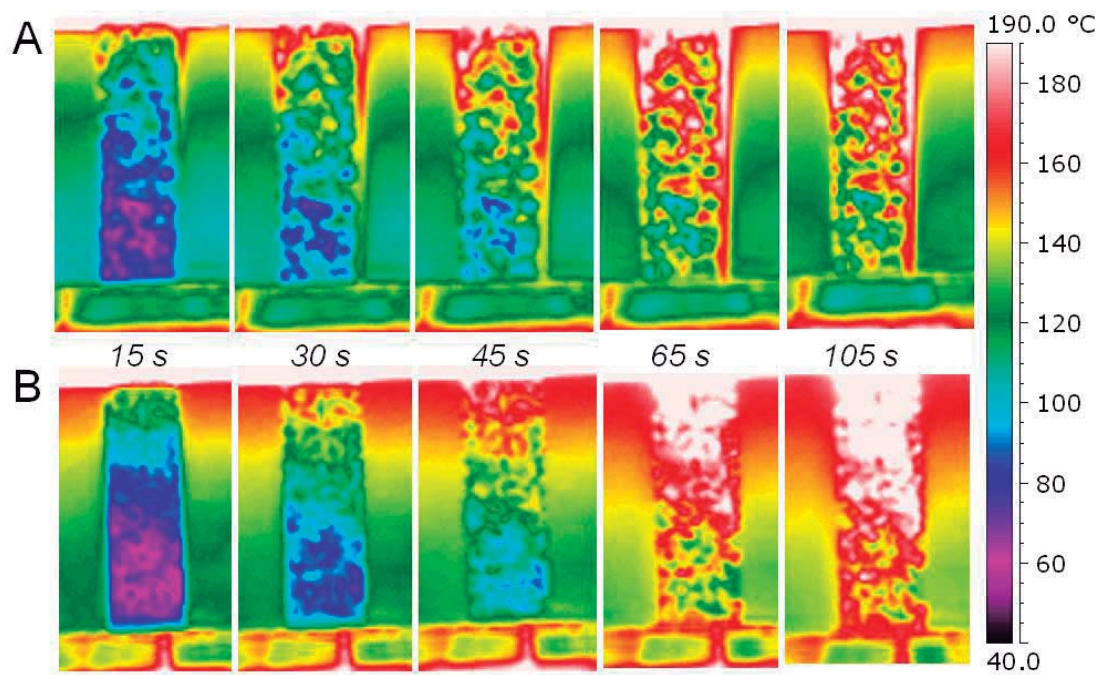


Figure 5. Thermographic images captured by infrared camera. (A) Sintered alloy sample. (B) Sample of a cast iron. The heating was performed from the top side by a preheated steel mass at 500°C. The dimensions of the sample were 11x11x40 cm.

In fact, the thermal coefficient of conductivity of cast iron varies between 58-47 ($\text{W}\cdot\text{m}^{-1}\cdot\text{K}^{-1}$) from 100 to 500°C. That of the sintered alloy can be approximated by considering the different constituents and the presence of porosity. In fact, sintered alloy has a high amount of porosity and therefore reduces the effective cross-section of the sample, and therefore heat is transmitted through the neck between the sintered particles... A complex mechanism of convection heat transmission occurs in the pores, but with lower heat transmission. In addition, the heterogeneous microcomposition diminished the thermal conductivity. The measured density values of the cast iron was $\rho_c = 7.71 \text{ gcm}^{-3}$, while sintered alloy had a $\rho_s = 6.05 \text{ gcm}^{-3}$. Considering the thermal conductivity of the different constituents of the sintered alloy, their proportions and the relative density (to take porosity into account) and following calculations as from ref. [13] a thermal conductivity variation of about 73 to 43 ($\text{W}\cdot\text{m}^{-1}\cdot\text{K}^{-1}$) again from 100 to 500°C for the sintered alloy is obtained. Thus, lower temperature dissipation at higher temperatures could be expected for the alloy as measured by the thermal experiments by infrared imaging.

Furthermore, in order to study the effect of temperature on the shear strength value, a standard shear test procedure was carried out at room temperature and at 500°C. Shear strength of a material may be an estimation of the probability of a possible failure when this material is working under shear loads, as in the case of shoe brake. The maximum friction force value would be reached at the shear strength value of the material.

Experiment results showed a sintered alloy shear strength of $\tau_s = 35 \text{ MPa}$ at 25°C, whereas at 500°C, τ_s decreased to 17 MPa. However, gray cast iron showed 160 MPa at 25°C and 100 MPa at 500°C. From these results, it can be predicted that sintered alloy

will wear by shear cutting before cast iron when high pressures and temperatures are reached.

4. Discussion

Cast iron kinetic friction coefficient curves showed that lower friction was measured for higher speeds and forces. Also, for this material, friction depended on the brake distance. However, the brake wear was higher in the sintered alloy. A μ loss measured when the force was increased, was observed in both shoe materials. Our experience in railway brake systems showed us that, in the range of pressures applied, friction force, F_c , shows a linear increase until a value at which the curve is cushioned as shown in figure 6. Under low contact pressures, the coefficient of friction is constant ($P_b < P_{b0}$), and follows equation 1:

$$\mu = \frac{F_b}{F} = \text{tg} \alpha \quad (\text{Eq. 1})$$

However, when the pressure reaches P_{b0} , a cushioned behavior is observed. At this pressure range:

$$F_b = C_i \cdot P_a^{n_p} \cdot S \quad (\text{Eq. 2})$$

, n_p being a coefficient of pressure with a value less than one. C_i is a constant of friction which depends on the topography of the surfaces in contact. Thus, the friction coefficient is a cushioned function guided by:

$$\mu = \frac{F_b}{F} = \frac{C_i \cdot P_b^{n_p} \cdot S}{P_b \cdot S} = C_i \cdot P_b^{-(1-n_p)} \quad (\text{Eq. 3})$$

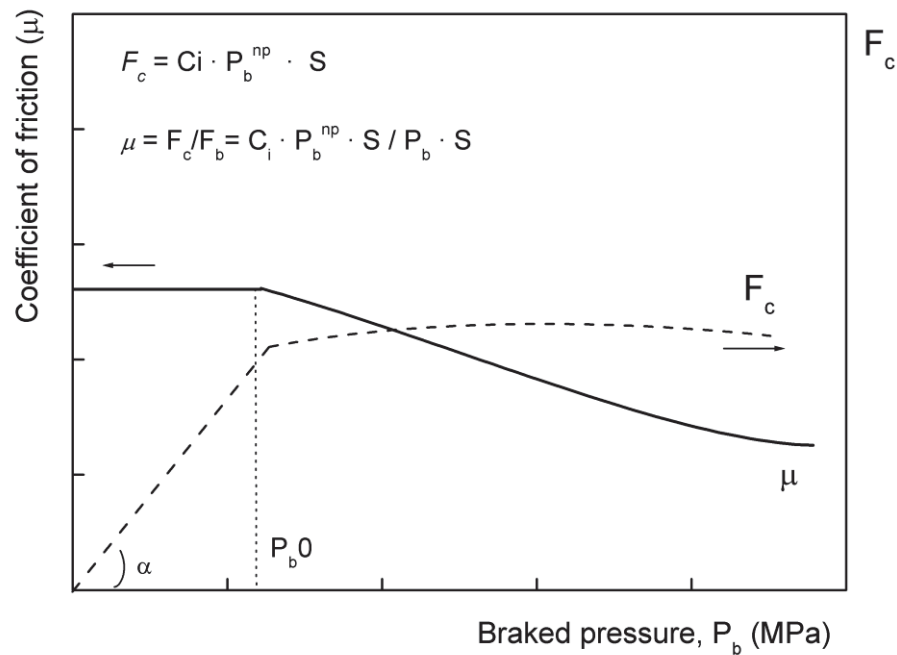


Figure 6. Cushioned function of the friction force when an increase in braking force is applied to the contact surface and μ , result of this function.

The mechanisms occurring on the contact area when a cushioned function is observed are due to the plastic deformation of the surface. The crests which form the roughness are deformed, thus changing the real contact surface. In fact, calculation of plasticity indexes as proposed by Greenwood and Williamson [14] yielded results well above the lower limit for considering plastic behavior. In order to calculate the local temperature increase in the irregularities, Archard's approach is followed [15]. According to this, to calculate flash temperature of the sliding pairs, apart to know whether the materials behaves elastically or plastic, slow and fast moving contacts have to be distinguished. For this purpose an non-dimensional parameter L considering speed, contact radius and properties of the materials is calculated. Unfortunately for the parameters and materials used in this work the results fall in between both regimes (L values vary from 0.32 to

1.55 for both materials, being in between the maximum value of 0.1 to be considered low speed, and the minimum value of 5 to be considered high speed. Nevertheless the temperatures are calculated considering low speed and plastic conditions as a first approximation. The results are presented in table 1:

| | V=0.3 m/s | | V=1 m/s | |
|----------------|-----------|-------|---------|-------|
| | F=10N | F=20N | F=10N | F=20N |
| Grey cast iron | 121°C | 98°C | 375°C | 273°C |
| Sintered alloy | 58°C | 73°C | 350°C | 456°C |

Table 1. Flash temperatures as calculated from Archard's equations

These results are well in agreement with the temperatures measured by the thermocouple, taking into account that these the calculated temperatures refer to the flash temperatures at the irregularities in the contact area whereas measured temperatures are about 10 mm away of this area in the pin.

A wide range of experiments must be performed to establish the critical force at which plastic deformation occurs, to determine the point at which μ begins to decrease in brake shoes. This should be matter of further research work.

The average increase of μ at higher velocities in the sintered alloy is thought to be due to the cohesive behavior of Cu rich phase. When temperature increases on the contact surface at high speeds, as inferred both by the measured temperatures and the flash temperatures worked out, this phase is more cohesive with the wheel. At low

temperatures, graphite is responsible for maintaining the lubrication to prevent welding between the brake and wheel. However, when graphite is released by increased temperature, due to frictional power, lubrication diminishes, increasing μ and temperature. Heat is not well dissipated through the shoe as shown in the infrared images. Thus, the shear strength limit of the brake surface decreases. As the shear strength limit is not very high for this material ($\tau_s = 35$ MPa at 500°C) metal is then released and wear in the brake pad is produced. This is the suspected reason for which sintered alloy presented a high level of wear at high velocities. Indeed, cast iron, which presented high shear strength values and good thermal conductivity, showed less wear. Regarding the reduced friction at higher sliding velocities in the case of grey cast iron, this behavior can be explained in terms of reduction of the ploughing term of friction [16-24] for increased velocities.

On the other hand, the higher wheel roughness observed when the cast iron sample was tested can be explained by the scratching of hard particles detached from the brake contact area. Usually, gray cast iron brake shoes contain titanium carbide particles in order to reduce wear [25]. These hard particles, together with other hard released material, are the cause of the major erosion produced in the wheel, and are therefore the cause of major rolling noise.

5. Conclusions

Pin-on-disc has been a useful technique for the measurement of the coefficient friction, μ , for one brake shoe made with cast iron and another made with a sintered copper alloy in contact with a standard railway wheel material. Although technique did not represent the actual conditions of the wheel-brake systems, the results obtained showed

interesting different behavior of both materials studied. These differences were resumed as:

1.- Sintered alloy has a constant and 80% higher friction coefficient compared to the cast iron shoe.

2.-Friction coefficient decreases with sliding friction velocity in cast iron shoes but increases this value in the sintered alloy. This behavior must be taken into account when high velocity train designs are being considered.

3.- The premature wear of sintered alloy occurred at high velocities due to the decrease in shear strength, an effect increased by the low thermal conductivity. However, the softer particles abraded from the sintered shoe produced a lower level of roughness on the wheel in comparison to cast iron, therefore being a better material in the policy to reduce the noise of the railway transport versus a higher wear.

Acknowledgements

We would like to thank the R&D&I Linguistic Assistance Office, Universidad Politécnica de Valencia (Spain), for translating this paper.

6. References

- [1] A. Lundström, M. Jäcker-Cüppers, P. Hübner, The new policy of the European Commission for the abatement of railway noise. *J. Sound and Vibration* 267 (2003) 397–405
- [2] P. De Vos. How the money machine may help to reduce railway noise in Europe. *J. Sound and Vibration* 267 (2003) 439–445
- [3] Tomaz Sedmak, Bojan Rosi, Vesna Smaka Kincl, Basic tools for controlling rolling noise in railway traffic, *Logistics & Sustainable Transport*, 1 (2) (2001)
- [4] M. Kalivoda, U. Danneskiold-Samsøe, F. Krüger, B. Barsikow. *Journal of Sound and Vibration* 267 (2003) 387–396
- [5] M. Macnaughta, Cast iron brake discs, a brief history of their development and metallurgy, Technical Report, Foundryman, (1998) 321.
- [6] S. Bühler, Methods and results of field testing of a retrofitted freight train with composite brake blocks, *J. Sound and Vibration* 293 (2006) 1041–1050
- [7] W. Österle and I. Urban, Friction layers and friction films on PMC brake pads, *Wear* 257 (2004) 215–226
- [8] Filip P., Weiss Z. and Rafaja D. On friction layer formation in polymer matrix

composite material for brake application, *Wear* 252 (2002) 189-198

[9] X. Xiang, S. Hong-chao, C. Jie, Y. Ping-ping, Effects of sintering pressure and temperature on microstructure and tribological characteristic of Cu-based aircraft brake material, *Trans. Nonferrous Met. Soc. China* 7 (2007) 669-675

[10] Maurice I. Ripley, Oliver Kirstein, Residual stresses in a cast iron automotive brake disc rotor, *Physica B* 385–386 (2006) 604–606

[11] G. Cueva, A. Sinatora, W.L. Guessser, A.P. Tschiptschin, Wear resistance of cast irons used in brake disc rotors, *Wear* 255 (2003) 1256–1260

[12] D. Bettge, J. Starcevic, Topographic properties of the contact zones of wear surfaces in disc brakes, *Wear* 254 (2003) 195-202

[13] L.J. Gibson, M.F. Ashby, *Cellular Solids*, 2nd edition, Cambridge University Press, (1997) 284-292

[14] J.A. Greenwood and J.B.P. Williamson, Contact of Nominally Flat Surfaces, *Proc. Roy. Soc., London, Series A*, 295 (1966) 300-319

[15] J.F. Archard, *Wear*, 2, 6 (1959) 438-455

[16] D. Tabor, *Tribology International*, 28, 1 (1995) 7-10

[17] F.P. Bowden and D. Tabor, *The Friction and Lubrication of Solids*, Clarendon Press, Oxford (1953) 98-100

[18] E. Orowan, The Calculation of roll pressure in hot and cold flat rolling. *Proc. Inst. Mech. Eng.* 150 (1941) 140-167

[19] C.M. Edwards and J. Halling, An analysis of the plastic interaction of surface asperities and its relevance to the value of the coefficient of friction . J. Mech. Phys. Solids 10 (1968) 101-110

[20] J. McFarlane and Tabor, Relation between friction and adhesion, Proc. Roy. Soc. 202A (1950) 244-253

[21] D. Tabor, Junction growth in metallic friction: the role of combined stresses and surface contamination, Proc. Roy. Soc. 251A (1958) 378-393

[22] A.P. Green, The plastic yielding of metal junctions due to combined shear and pressure. J. Mech. Phys. Solids 2 (1954) 197-211

[23] A.P. Green, Friction between unlubricated metals: a theoretical analysis of the junction model, Proc. Roy. Soc. 228A (1955) 191-204

[24] Bharat Bhushan. Principles and Applications of Tribology. (1999) 978-0-471-59407-9

[25] B.J. Chapman, G. Mannion, Titanium-bearing cast iron for automotive braking applications, J. Foundry Trade 152:3732 (1982) 232-234